## Original Article

# The protective effects of human umbilical cord mesenchymal stem cells on damaged ovarian function: A comparative study

Jinjin Zhang[1], Jiaqiang Xiong[1], Li Fang[1], Zhiyong Lu[1], Meng Wu[1], Liangyan Shi[2], Xian Qin[1], Aiyue Luo[1], Shixuan Wang[1,*]

[1] *Department of Obstetrics and Gynecology, Tongji Hospital, Huazhong University of Science and Technology, Wuhan, Hubei, China;*
[2] *Department of Obstetrics and Gynecology, Hubei Province, Maternity and Child Health Care Hospital, Wuhan, Hubei, China.*

**Summary**      **Numerous studies have reported that human umbilical cord mesenchymal stem cell (hUCMSC) therapy can rescue the structure and function of injured tissues. The aims of this study were to explore the protective role of hUCMSC transplantation in a model of accelerated ovarian aging and to compare 2 methods of transplanting hUCMSCs, *i.e. i*) via intravenous injection (IV) and *ii*) in situ ovarian micro injection (MI). Female mice were subjected to superovulation and ozone inhalation to create a model of accelerated ovarian aging with a decline in both the quantity and quality of oocytes. Cells were transplanted *via* IV or MI, and ovaries were removed after 2 weeks or 1 month of treatment. Ovarian reserve and function were evaluated based on the follicle counts, hormone levels, the estrous cycle, and reproductive performance. Cell tracking, terminal deoxynucleotidyl transferase-mediated dUTP nick end labeling (TUNEL), real-time polymerase chain reaction (PCR), and Western blot analysis were used to assess the inner mechanisms of injury and repair. Results indicated that ovarian function increased significantly after treatment with hUCMSCs. Immunofluorescence revealed reduced TUNEL staining and a decreased percentage of apoptotic cells. A higher level of expression of anti-apoptotic and antioxidant enzymes was noted in the ovaries of groups treated with hUCMSCs. These parameters were enhanced more when mice were treated with hUCMSCs for 1 month than when they treated with hUCMSCs for 2 weeks. IV was better able to restore ovarian function than MI. These results suggest that both methods of transplantation may improve ovarian function and that IV transplantation of hUCMSCs can significantly improve ovarian function and structural parameters more than MI transplantation of hUCMSCs can.**

*Keywords:* Ovarian aging, hUCMSCs, model of accelerated ovarian aging, intravenous injection, in situ ovarian micro injection

## 1. Introduction

Aging of the ovaries is characterized by a gradual decline in both the quantity and quality of oocytes. At the 16th-20th week of fetal development, the ovaries contain 6-7 million primordial follicles (*1,2*), which serve as a

*Address correspondence to:*
Dr. Shixuan Wang, Department of Obstetrics and Gynecology, Tongji Hospital, Huazhong University of Science and Technology, Wuhan, Hubei 430030, China.
E-mail: sxwang@tjh.tjmu.edu.cn

source of developing follicles (*1,3,4*). Unfortunately, the number of oocytes inevitably declines with age. At birth, approximately 1-2 million primordial follicles remain in the ovaries (*5*). By the onset of puberty, the number of primordial follicles declines to only 300,000 to 400,000 (*6,7*). At child-bearing age, the number of primordial follicles decreases steadily at a rate of about 1,000 follicles per month and drops below 1,000 at the average age of 51 years (menopause) (*8-10*).

As the follicle count decreases with age, oocyte quality also diminishes. The products produced by oxidative stress during daily metabolism may cause aging (*11*). Long-term greater oxidative stress damage may be involved in the process of ovarian aging (*12,13*). Previous

studies have indicated that oxidative stress harms oocyte development. A study that examined the relationship between oxidative stress and poor oocyte quality suggested that women who undergo IVF have a higher proportion of degenerative oocytes and a significantly higher level of 8-hydroxy-2'-deoxyguanosine (8-OHdG, a marker of the degree of DNA oxidation) in the ovarian follicular fluid (*14*). When women who failed to become pregnant after IVF were given antioxidants, they had a markedly lower level of 8-OHdG in the follicular fluid and a higher pregnancy rate. Recent studies have also suggested that mitochondrial dysfunction is involved in age-related damage to oocytes. The undesirable changes caused by excessive free radicals can result in cellular injury that increases with age (*15,16*). Along with an age-related decrease in estrogen levels, the absence of the beneficial effects of estrogen on oxidative stress finally causes damage to the ovaries. This may explain the significantly increase in the rate of congenital birth defects in women over age 38 (*17*). The accumulation of oxidative damage and an accompanying diminishing of antioxidant defenses will ultimately lead to ovarian aging.

Based on these findings, a new a model of accelerated ovarian aging was created to induce a decline in both the quantity and quality of oocytes by superovulation and ozone inhalation. Repeated ovulation was induced in mice by sequentially administering pregnant mare serum gonadotropin (PMSG), human chorionic gonadotropin (hCG), and prostaglandin F2α (PGF2α) to reduce the primordial follicle pool. Ozone inhalation was used to increase oxidative damage throughout the body, including the ovaries.

Previous studies have suggested that stem cells have the ability to differentiate into a variety of cell phenotypes, so they can be used to treat various diseases. Given this contention, suitable stem cells could most likely be used to delay ovarian aging. Stem cell therapy has been found to restore the fertility of patients, although its mechanism is unclear (*18*). Mesenchymal stem cells (MSC) derived from Wharton's jelly of the human umbilical cord (human umbilical cord MSCs, or hUCMSCs) have displayed characteristics similar to those of bone marrow mesenchymal stromal cells (BMSCs). Compared to BMSCs, hUCMSCs have many merits as a cell treatment because of their relatively large capacity for *ex vivo* expansion, low risk of viral infection, lack of donor morbidity, and less pronounced immunogenicity (*19-21*). Evidence has shown that hUCMSCs have unique advantages compared to BMSCs (*22*), which make them a promising source of cells for treatment. According to previous studies, stem cells to treat ovarian injury are primarily administered *via* intravenous injection (IV) or in situ ovarian micro injection (MI) (*23-26*). However, very few studies have examined suitable forms of hUCMSC therapy to delay ovarian aging. The current study sought to evaluate

2 different forms of hUCMSC therapy for protection against ovarian aging in an animal model in order to offer a better form of cell therapy.

## 2. Materials and Methods

This study was conducted in the Stem Cell Research Laboratory in Gynecology & Obstetrics. This study followed procedures consistent with the guidelines for the care and use of laboratory animals issued by the Academy of Tongji Medical College at Huazhong University of Science and Technology.

### 2.1. *Preparation, culture, and identification of hUCMSCs*

hUCMSCs were prepared, identified, and cultured according to a recently published protocol (*23*). At passage 6, the expression of cell surface markers was analyzed with flow cytometry using fluorescein isothiocyanate (FITC)-conjugated human monoclonal antibodies such as CD14 (BioLegend, 325623), CD31 (BioLegend, 303103), CD34 (BioLegend, 343603), CD105 (BioLegend, 323203), CD45 (BioLegend, 304005), CD44 (BioLegend, 338803), CD73 (BioLegend, 344015), human leukocyte antigens-D region (HLA-DR, BioLegend, 307603), phycoerythrin (PE)-conjugated human antibodies against CD90 (BioLegend, 328109), and PE-CD29 (BioLegend, 303003). Adherent cells were detached by treatment with 0.25% trypsin ethylene diamine tetraacetic acid (EDTA) and incubated with monoclonal antibodies, re-suspended in 0.4mL phosphate buffer solution (PBS), and immediately analyzed using a flow cytometer. To further detect the differentiation potential of hUCMSCs, osteogenic and adipogenic experiments were conducted, and alkaline phosphatase (ALP) and oil red O staining were used to indicate differentiation.

### 2.2. *Creation of an animal model*

Female C57BL/6 mice (6 weeks old, weighing 16.7 ± 0.8 g) were obtained from Beijing HFK Bio-Technology (Beijing, China). All mice were housed in a specific pathogen-free (SPF)-grade facility with a controlled temperature (25°C) and light cycle (12 h light, 12 h dark). To create a model of accelerated ovarian aging, mice were super-ovulated *via* an intraperitoneal injection of 5 IU of pregnant mare serum gonadotropin (PMSG) (Hangzhou Animal Medicine Factory, Hangzhou, China). Forty-eight hours after PMSG administration, the mice were intraperitoneally administered 5 IU human chorionic gonadotropin (hCG) (Livzon Pharmaceutical Group Inc., Guangzhou, China); 19 hours later, 25 IU of PGF2α (Hangzhou Animal Medicine Factory, Hangzhou, China) was administered intraperitoneally. Five hours after PGF2α administration, the sequential administration of the

three agents was repeated 10 times in 30 days (*27*). To induce ozone inhalation, mice were placed in a half-open system in which an ozonator (manufactured by Beijing Kang Er Xing Technology Development Co. Ltd., Beijing, China) had been placed on a rack. An ozone meter (manufactured by Beijing Kang Er Xing Technology Development Co. Ltd., Beijing, China) was used to measure the ozone concentration inside the cage during the experiment. Once the ozonator was turned on, the fresh airflow that entered the ozonator was regulated to maintain the ozone concentration in the center of the cage at 1.2 mg/m$^3$ (*28,29*). The mice were exposed to ozone for 8 h (20:00-04:00) each day until the end of the last cycle of superovulation. A photograph of intraperitoneal injection and a diagram of the ozone chamber are shown in Figure 1.

### 2.3. Animal groups

One hundred and twenty-six mice were randomly divided into 2 groups. The normal control group (NC, *n* = 12) consisted of untreated normal mice and the model group (Mod, *n* = 114) consisted of mice with accelerated ovarian aging. Once the model was created, 6 mice from each group were sacrificed to assess ovarian function. The remaining mice were divided into 8 groups: IV-u2w, IV-p2w, MI-u2w, MI-p2w, IV-u1m, IV-p1m, MI-u1m, and MI-p1m. Each group consisted of 12 mice.

### 2.4. PKH26 labelling

hUCMSC membranes were labeled with a lipophilic dye, PKH26, usong the PKH26 Red Fluorescence Kit (Sigma-Aldrich) according to the manufacturer's instructions (*30*). The labeled cell suspension was diluted to almost $1 \times 10^6$ cells/mL. The collected cells were then stained with trypan blue to ensure cell viability was over 95%. Cells were then used for cell therapy.

### 2.5. hUCMSC transplantation

Mice in the IV-u2w and IV-u1m groups were administered hUCMSCs *via* the tail vein for 2 weeks and 1 month, respectively, and the IV-p2w and IV-p1m groups were treated with PBS. As shown in Figure 2, mice in the intravenous group (IV-u2w, IV-u1m) were injected intravenously with $1 \times 10^6$ hUCMSCs in 100 μL of PBS as described in previous studies (*31-33*). Mice in the IV-p2w and IV-p1m groups were injected with 100 μL of PBS alone. The same amount was injected the following day. In the IV-u1m group and IV-p1m group, PBS was injected again 15 and 16 days after the first injection.

In the in situ micro injection groups (MI-u2w and MI-u1m), a total of $2 \times 10^6$ hUCMSCs in 10 μL of PBS was injected directly into the bilateral ovaries with
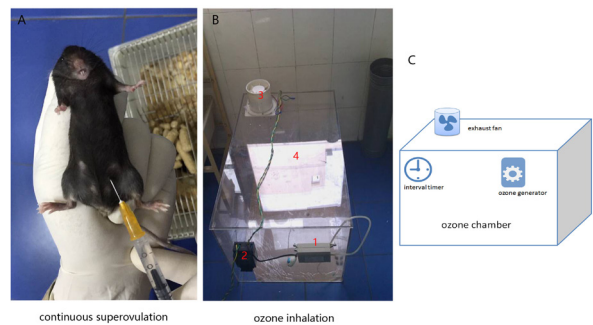


**Figure 1. Model setup. (A)** Intraperitoneal injection. **(B)** Ozone inhalation. **(C)** Diagram of the ozone chamber. *Note*: 1. Ozone generator; 2.Timer; 3. Exhaust fan; 4. Ozone chamber.
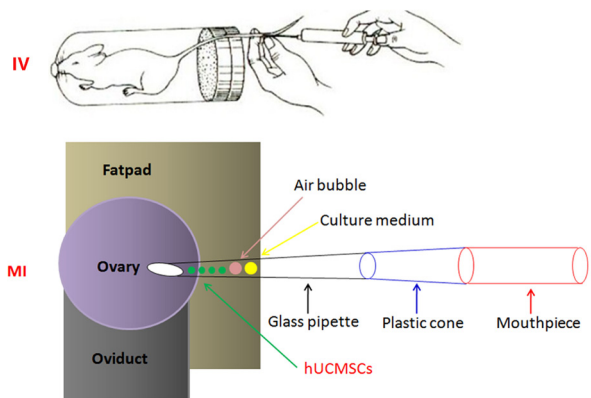


**Figure 2. hUCMSC transplantation.** IV: Intravenous injection; MI: In situ ovarian micro injection.

a micro injector while mice in the MI-p2w and MI-p1m groups were injected with 10 μL of PBS alone to serve as a control. No leakage was apparent after transplantation.

### 2.6. Ovarian follicle counts and morphological analysis

Two weeks or 1 month after cell transplantation, 6 mice from each group were sacrificed and their ovaries were removed and fixed for sectioning. Mouse ovaries fixed in 4% paraformaldehyde for 24 h were transferred to 70% ethanol, embedded in paraffin, and successively cut lengthwise into sections of 5 μm. Every fourth section was mounted on a glass slide. Ever other slide was stained with hematoxylin and eosin and analyzed under a microscope by 2 researchers who were blinded to the origin of the sections. Only follicles containing oocytes with a nucleus were scored in histomorphometric evaluation, as originally described (*34*). In all sections, the numbers of primordial, growing, and antral follicles were tallied to obtain the count of each type of follicle in a given ovary.

### 2.7. Hormone examination

Sterile non-heparinized tubes were used to collect blood samples from non-pregnant mice during the diestrus

of the estrous cycle in sterile non-heparinized tubes. The blood samples were centrifuged at 3,000 rpm for 5 minutes, and serum was collected and stored at -80°C until analysis. Levels of serum E2 and P were measured using an enzyme-linked immune sorbent assay (ELISA) according to the manufacturer's instructions (Cayman Chemical Company, Ann Arbor, MI, USA).

### 2.8. Estrous phase and fertility tests

Five mice in each group were used in estrous cycle and fertility tests. The estrous cycles of the female mice were regularly assessed every morning between 08:00 and 9:00 AM using vaginal cytology (*35,36*). Mating trials were initiated 20 days after hUCMSC treatment and lasted for 4 months. The number and survival rate of fetuses and the time of birth were recorded to evaluate reproductive performance.

### 2.9. Detection of apoptosis

Apoptotic cells in ovarian tissue sections were identified with an in situ Cell Death Detection Kit, POD (Roche, Germany) according to the manufacturer's instructions. Paraffin sections of the ovaries were dewaxed, rehydrated, digested with proteinase K (10 μM) for 5 min, incubated in TUNEL enzyme (10% v/v; Roche) and TUNEL label (90% v/v; Roche) for 60 min at 37°C, and mounted in ProLong Gold medium containing 4',6-diamidino-2-phenylindole (DAPI). Negative control sections were incubated with a TUNEL reaction mixture without enzyme (terminal deoxynucleotidyl transferase, TdT). Finally, the sections were observed and digital images were recorded using a Leica inverted SP5 confocal laser-scanning microscope (Leica Microsystems, Wetzlar, Germany).

### 2.10. Real-time fluorescence quantitative polymerase chain reaction (qPCR)

Total RNA in the ovaries was extracted. Real-time PCR was performed using the AB StepOne Plus PCR machine (Applied Biosystems, Foster City, CA, USA) as described in a previous study (*37*). The PCR amplification of all transcripts was performed with the gene-specific primers listed in Table 1. Primers were found in the literature or designed with software Primer 3.0. The quality and identity of each PCR product was determined using melting curve analysis. The expression of mRNA was calculated using the delta-delta Ct method, with relative gene expression = $2^{-(\Delta Ct\,sample - \Delta Ct\,control)}$ (*38*). All data were normalized to expression of glyceraldehyde-3-phosphate dehydrogenase (GAPDH).

### 2.11. Western blot analysis

Western blot analysis was performed as previously

described (*39*). Cell membranes were incubated overnight at 4°C with a primary antibody against superoxide dismutase 2 (SOD2, Abcam, UK, ab13533, 1:5,000 dilution), catalase (CAT, Abcam, UK, ab16731,1: 2,000 dilution), Bcl-2 associated X protein (Bax, Abcam, UK, ab32503, 1: 5,000 dilution), Bcl2 (Abcam, UK, ab32124, 1:1,000 dilution), or β-actin (Sigma,1: 1,000 dilution). Afterwards, membranes were incubated with a horseradish peroxidase-conjugated anti-rabbit or antimouse antibody (1:3,000 dilution) for 30 minutes at room temperature and washed 3 times with tris-buffered saline tween20 (TBST). After incubation with a chemiluminescent substrate for 5 minutes, protein signals were detected with BIO-RAD ChemiDoc™ XRS (USA) and analyzed with Image Lab™ Software.

### 2.12. Statistical analysis

Statistical analysis was performed using the software SPSS®17.0 with data expressed as the mean ± SEM. Student's t-test was used to compare the NC and Mod groups to assess the model. One-way analysis of variance (ANOVA) was used to compare hormones, follicle counts, apoptosis rates, and gene expression among the groups. Differences in estrous cycles were evaluated using ANOVA with a post-hoc Tukey's test. Values with $p < 0.05$ were considered to indicate a significant difference.

## 3. Results

### 3.1. Characterization of hUCMSCs

At least 10 days was needed for the first colonies of hUCMSCs to appear, and an extra week was required for them to reach 50-60% confluency. Isolated hUCMSCs in culture were characterized using microscopy and flow cytometry. The morphology of cultured hUCMSCs resembled fibroblasts with few other cells (Figure 3A). To determine the extent to which induction resulted in hUCMSC differentiation into adipocytes versus osteoblasts, the cells were examined with oil red O and ALP staining. As shown in Figure 3B and 3C (red cells), isolated hUCMSCs were able to differentiate into both adipocytes and osteoblasts. In addition, flow cytometry was used to recognize the expression of surface markers at passage 6. Results indicated that the cultured hUCMSCs were negative for HLA-DR, CD14, CD31, CD34, and CD45. However, more than 95% of the cell population was positive for the markers CD29, CD44, CD73, CD90, and CD105 (Figure 3D).

### 3.2. Assessment of the animal model

In order to assess whether the mouse model of accelerated ovarian aging was effectively created, ovarian morphology, ovarian follicle counts, plasma estrogen

**Table 1. List of specific primers and amplification conditions for real-time PCR**

| NCBI accession | Aliases | Sequence (5'-3') | | Tm, Cycles | Size (bp) |
| | | Forward | Reverse | | |
|---|---|---|---|---|---|
| NP_032110 | GAPDH | AAGGGTGGAGCCAAAAGGG | GGGGGCTAAGCAGTTGGTG | 60, 30 | 141 |
| NP_031553 | Bax | CCCGAGAGGTCTTCTTCCG | AGCCGCTCACGGAGGAAGT | 60,30 | 181 |
| NP_803129 | Bcl2 | GATGCTGGAGATGCGGACG | ACGACGGTAGCGACGAGAG | 60,30 | 240 |
| NP_033934 | CAT | GGAGGCGGGAACCCAATAG | GTGTGCCATCTCGTCAGTGAA | 60,30 | 102 |
| NP_038699 | SOD2 | CAGACCTGCCTTACGACTATGG | CTCGGTGGCGTTGAGATTGTT | 60,30 | 113 |
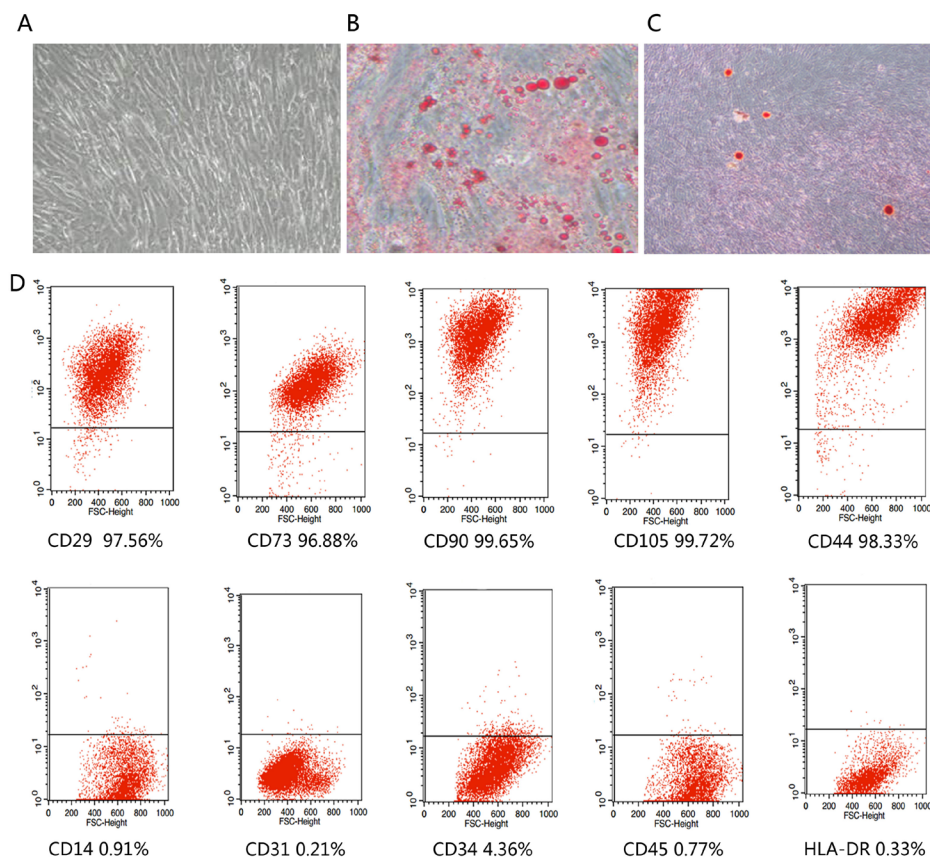


**Figure 3. Isolation and identification of hUCMSCs. (A)** hUCMSCs have a typical fibroblastic morphology. **(B)** hUCMSCs differentiate into adipocytes. **(C)** hUCMSCs differentiate into osteoblasts. **(D)** Flow cytometry analysis of hUCMSCs. Cells were positive for CD29, CD90, CD105, CD73, and CD44 and negative for CD14, CD31, HLA-DR, CD34, and CD45.

and progesterone levels, and reproductive performance were studied. Once the model was created, examination of the ovaries indicated that the ovaries of the NC mice contained numerous follicles in each stage. However, the ovaries of the mice in the Mod group mostly consisted of secondary follicles and atretic follicles, with fewer primordial follicles and primary follicles. Moreover, the plasma levels of estrogen and progesterone decreased, along with fertility, in the Mod group compared to levels in the NC group. These results indicated that the Mod group of mice had diminished ovarian reserve. The specific results are shown below.

### 3.3. hUCMSCs restored ovarian function in terms of both ovarian follicle counts and morphology

Two weeks after PKH26-labeled hUCMSCs were intravenously injected, those cells were tracked in mouse ovaries. However, the labeled cells did not develop into follicles or oocytes. Follicles stained with hematoxylin and eosin in each stage in all groups are shown in Figure 4A-J. Female mice who were super-ovulated and subjected to ozone inhalation exhibited physiological ovarian aging. The NC group of mice had $61.5 \pm 10.3$ primordial follicles, and the Mod group of mice had $38.0 \pm 7.1$ primordial follicles (Mod *vs.* NC, $p < 0.01$). There were fewer primordial and primary follicles in the ovaries of the mice in the Mod group than in the NC group. Moreover, the number of secondary follicles and atretic follicles in the Mod group was higher than that in the NC group ($p < 0.01$ for secondary follicles and $p < 0.05$ for atretic follicles).

The hUCMSCs were administered intravenously or *via* in situ micro injection. Ovaries were removed
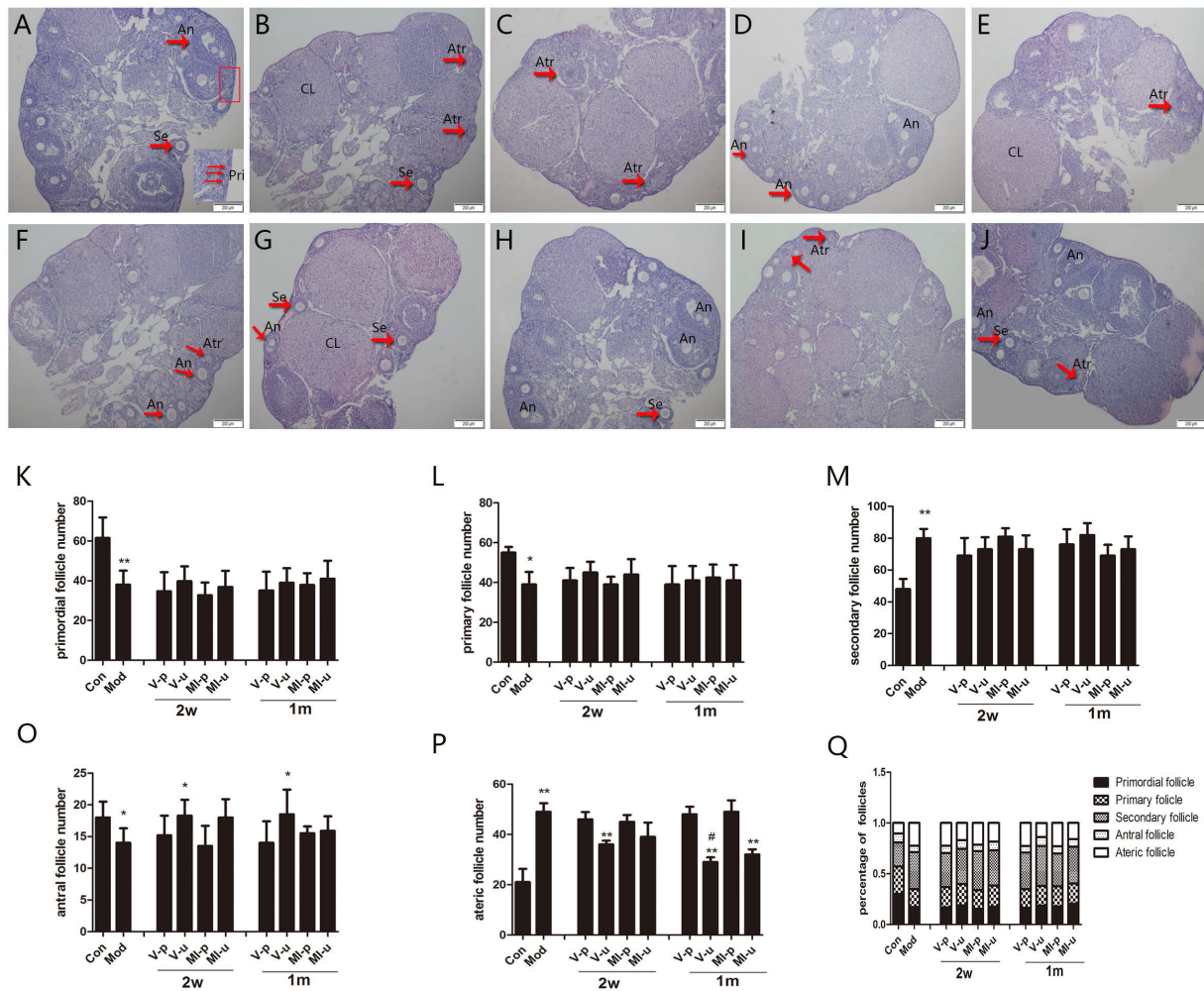
**Figure 4. The effect of transplantation on follicle morphology and number in each group during various stages of development. (A-J)** Representative histological images of the ovaries in each group of mice. Once the model was created, the ovaries of the Mod group had fewer primordial and primary follicles compared to the NC group. However, the number of secondary follicles and atretic follicles in the Mod group increased significantly. Atretic follicles decreased and healthy antral follicles increased after treatment with hUCMSCs for 2 weeks or 1 month. Bar = 200 μm; Pri: primordial follicles; Se: secondary follicles; An: antral follicles; Atr: atretic follicles; CL: corpus luteum. **(K-Q)** Numbers of each grade of follicles in all groups. **(K)** Primordial follicles. **(L)** Primary follicles **(M)** Secondary follicles **(O)** Antral follicles **(P)** Atretic follicles. **(Q)** The percentage of follicles in each group during various stages. The * symbol represents the Mod group versus the NC group or groups treated with hUCMSCs versus corresponding groups treated with PBS, *$p < 0.05$, **$p < 0.01$; The # symbol represents IV-u1m group versus IV-u2w group, #$p < 0.05$.

2 weeks or 1 month after treatment, and the number of each type of follicle was determined. Ovaries from mice that were treated with hUCMSCs (IV-u2w, IV-u1m, MI-u2w, and MI-u1m) had similar numbers of primordial follicles, primary follicles, and secondary follicles in comparison to the Mod group of mice and the corresponding groups treated with PBS (Figue 4K-M) ($p > 0.05$). Groups treated with hUCMSCs had a greater number of healthy antral follicles than did groups treated with PBS except for the MI-u2w and MI-u1m groups. After treatment, however, atretic follicles decreased in the IV-u2w, IV-u1m, and MI-u1m groups compared to the corresponding groups treated with PBS. The follicle count did not differ significantly in the IV-u1m group or the IV-u2w group except in terms of the number of atretic follicles. Nevertheless, the atretic follicle count decreased substantially with the duration of hUCMSC treatment in the IV-u1m group than in the IV-u2w group. As shown

in this study, 1 month may be the optimal duration of stem cell therapy. The number and percentage of follicles in each group during various stages of development are shown in Figure 4K-Q.

### 3.4. *hUCMSCs restored ovarian function in terms of sex hormone levels*

Follicular development was evaluated in all groups by monitoring estrous cycles with vaginal smears, and estrogen and progesterone levels in serum were measured. Two weeks or 1 month after hUCMSC treatment, the serum levels of estrogen and progesterone in the treated groups increased significantly compared to those in the corresponding groups treated with PBS ($p < 0.05$). Levels of estrogen and progesterone did not differ significantly in the MI-p2w group or the MI-u2w group. Estrogen levels in mice increased with the
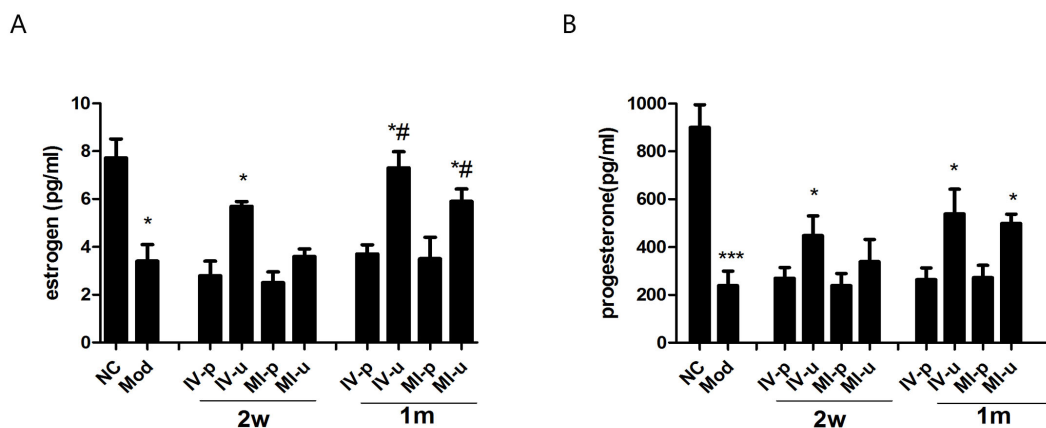
A



B



**Figure 5. Estrogen and progesterone levels in different groups.** After hUCMSC treatment, serum levels of estrogen **(A)** and progesterone **(B)** increased significantly compared to levels in the corresponding groups treated with PBS, and those levels did not differed significantly in the MI-u2w group and the MI-u2w group. The * symbol represents the Mod group versus the NC group or groups treated with hUCMSCs versus corresponding groups treated with PBS, $*p < 0.05$, $***p < 0.001$; The $^{#}$ symbol represents the IV-u1m group versus the IV-u2w group or the MI-u1m group versus the MI-u2w group, $^{#}p < 0.05$.

**Table 2. Effect of hUCMSCs on the estrous cycle ($n = 5$) and reproductive performance ($n = 5$)**

| Reproductive performance | NC | Mod | IV-p2w | IV-u2w | MI-p2w | MI-u2w | IV-p1m | IV-u1m | MI-p1m | MI-u1m |
|---|---|---|---|---|---|---|---|---|---|---|
| Regular cycles (%) | 100 | 0 | 0 | 25 | 0 | 12.5 | 0 | 37.5 | 0 | 25 |
| Irregular cycles (%) | 0 | 37.5 | 25 | 37.5 | 12.5 | 25 | 37.5 | 50 | 50 | 37.5 |
| Cessation of cycle (%) | 0 | 62.5 | 75 | 37.5 | 87.5 | 62.5 | 62.5 | 12.5 | 50 | 37.5 |
| Total number of newborns ($n$) | 51 | 37 | 39 | 47 | 41 | 45 | 38 | 49 | 41 | 51 |
| Mean litter size ($n$) | $10.2 \pm 1.5$ | $7.4 \pm 1.3^*$ | $7.8 \pm 2.1$ | $9.4 \pm 1.0$ | $8.2 \pm 0.6$ | $9 \pm 1.1$ | $7.6 \pm 0.9$ | $9.8 \pm 1.7^*$ | $8.2 \pm 2.1$ | $10.2 \pm 1.6^*$ |
| Gross survival rate (%) | 100 | 95.1 | 89.7 | 91.7 | 92.6 | 93.3 | 94.7 | 98.0 | 95.1 | 96.1 |

duration of treatment and differed significantly in groups treated with hUCMSCs for 1 month or 2 weeks (the MI-u1m group *vs.* the MI-u2w group, $p < 0.05$; the IV-u1m group *vs.* the IV-u2w group, $p < 0.05$) (Figure 5A-B). The levels of progesterone in the IV-u2w, IV-u1m, and MI-u1m groups increased significantly compared to the corresponding groups treated with PBS. Similar to estrogen, progesterone levels did not differ in the MI-u2w group or MI-p2w group.

### 3.5. hUCMSCs restored the estrous cycle and reproductive performance

All mice in the NC group exhibited a regular 4-5-d estrous cycle and each phase of the estrous cycle had a normal length. Once the model was created, the mice displayed a prolonged estrous cycle with a significant increase in the duration of the metaestrus phase; 37.5% of mice had irregular cycles and 62.5% had cycles that ceased. Two weeks or 1 month after hUCMSC treatment, a significantly higher percentage of mice in the IV-u2w (25%), MI-u2w (12.5%), IV-u1m (37.5%), and MI-u1m (25%) groups had regular cycles compared to the corresponding groups treated with PBS, *i.e.* the IV-p2w (0%), MI-p2w (0%), IV-p1m (0%), and MI-p1m (0%) groups. Mice treated with hUCMSCs for 1 month were compared to those treated with hUCMSCs for 2 weeks. Results revealed that the percentage of mice with a

regular cycle increased with the duration of hUCMSC treatment, regardless of the method of transplantation (Table 2). The decline in fertility and fecundity is the most obvious outcome of ovarian aging, so the mean litter size and mean number of litters were analyzed in both groups after 4 months of breeding. Both the number of newborns per litter and the total number of litters decreased markedly in the Mod group ($7.4 \pm 1.3$; 37) compared to those in the NC group ($10.2 \pm 1.5$; 51). The pregnancy rate did not decrease significantly in any group (Table 2). Moreover, no external morphological abnormalities were noted in the offspring of the groups. Mice treated with hUCMSCs for 2 months had similar numbers of litters and numbers of newborns per litter compared to their counterparts, which suggests that short-term transplantation of hUCMSCs does affect the reproductive performance of mice. When female mice were treated with hUCMSCs for 1 month and mated with normal males of proven fertility, those females were significantly more fertile than the female controls. The number of newborns per litter and the total number of litters increase in the IV-u1m ($9.8 \pm 1.7$, 49) and MI-u1m ($10.2 \pm 1.6$, 51) groups in comparison to those in the IV-p1m ($7.6 \pm 0.9$, 38) and MI-p1m ($8.2 \pm 2.1$, 41) groups, which suggests that 1 month of treatment may be more suitable to restore fertility ($p < 0.05$) (Table 2). In addition, the pregnancy rate and survival rate were similar among the groups.
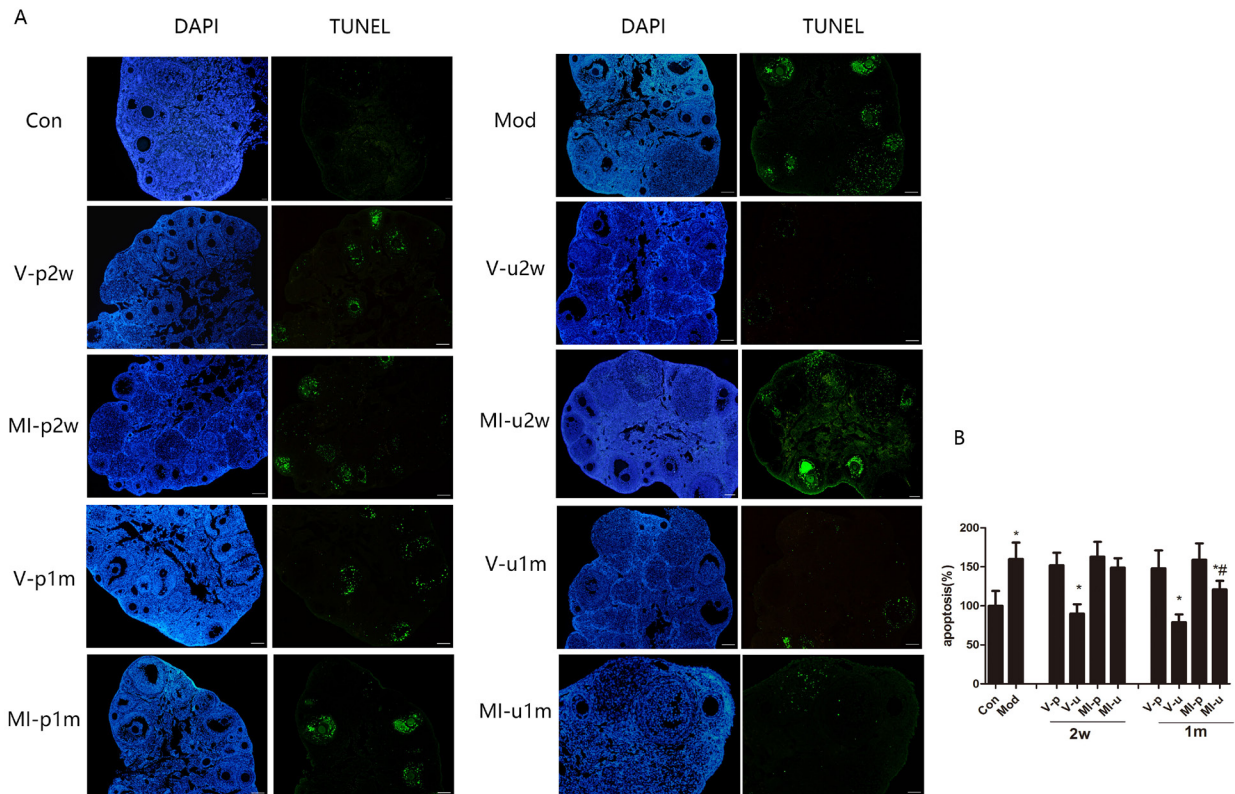
**Figure 6. Apoptosis in the ovaries decreased after hUCMSC treatment. (A)** Representative images of ovarian tissue obtained from all groups of mice. Data from 2 weeks and 1 month after hUCMSC treatment indicate that apoptosis was attenuated by the transplantation of hUCMSCs. Bar = 50 μm. **(B)** The rate of GC apoptosis in each group. Values are expressed as the mean ± SD. The * symbol represents the Mod group versus the NC group or groups treated with hUCMSCs versus corresponding groups treated with PBS, *$p < 0.05$; The # symbol represents the MI-u1m group versus the MI-u2w group, #$p < 0.05$.

### 3.6. *hUCMSCs reduced the apoptosis of granulosa cells*

Once the model was created, granulosa cells and other cells in the ovaries experienced dramatic apoptosis. Blue staining in the ovaries indicates the nucleus and green staining indicates TUNEL-positive GCs. The apoptosis of GCs in the Mod group was almost 1.5-fold of that in the NC group. Two weeks and 1 month after hUCMSC transplantation, the percentage of TUNEL-positive GCs in these 2 treated groups was significantly lower than that in groups treated with PBS, as shown in Figure 6A-B. The number of apoptotic GCs decreased after hUCMSC treatment (the IV-u2w group *vs.* the IV-p2w group, $p < 0.05$; the IV-u1m group *vs.* the IV-p1m group, $p < 0.05$; the MI-u1m group *vs.* the MI-p1m group, $p < 0.05$). The percentage of apoptotic cells decreased in the MI-u1m group compared to that in the MI-u2w group ($p < 0.05$) but did not differ significantly in the MI-u2w group or the MI-p2w group. Values are expressed as the mean ± SEM.

### 3.7. *hUCMSCs restored ovarian function via antioxidant and anti-apoptotic enzymes*

Gene expression in the groups treated with hUCMSCs was compared to that in the groups treated PBS, revealing that some genes that regulate antioxidant and anti-apoptotic action were altered. The groups treated with hUCMSCs expressed more SOD2, CAT, and Bcl2 mRNA and less Bax mRNA than did the groups treated with PBS (Figure 7). Levels of mRNA expression of some genes (SOD2 and Bcl2) were significantly higher in the IV-u1m group than in the MI-u1m group but those levels did not differ significantly in the IV-p1m group or the MI-p1m group (Figure 7A, D). The level of expression Bcl2 mRNA was much higher in the IV-u2w group than in the MI-u2w group ($p < 0.05$), as shown in Figure 7 D.

The level of protein expression was examined, revealing a trend like that observed with mRNA levels, as shown in Figure 8. Antioxidant and anti-apoptotic proteins increased and pro-apoptotic proteins decreased in the groups treated with hUCMSCs. hUCMSCs were found to restore ovarian function, and this observed effect was presumably due to high levels of antioxidant and anti-apoptotic enzymes since the ovaries did not form any oocytes or GCs. Hence, this action means that hUCMSCs are suitable for regenerative cell therapy.

### 4. Discussion

A woman's fertility is known to decline with age. The gradual loss of fertility becomes more prominent after the age of 35 and stops during menopause at a mean age of 50-51 years (*40*). The ovaries have accelerated aging
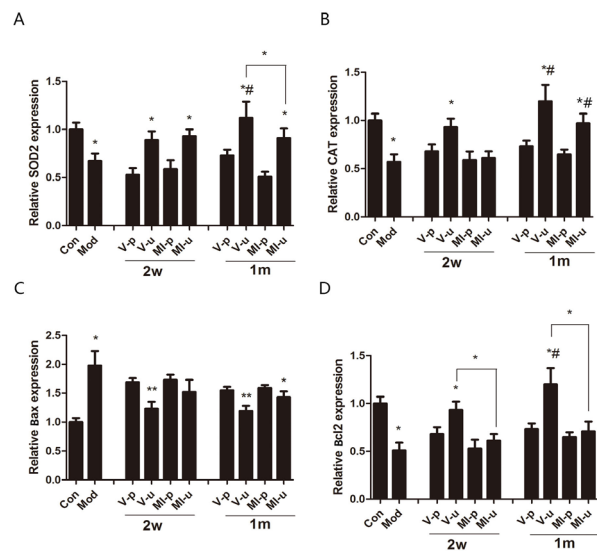
**Figure 7. Effects of hUCMSCs on expression of mRNA of genes coding for antioxidant and anti-apoptotic enzymes in ovaries.** Relative levels of expression of the genes SOD2 **(A)**, CAT **(B)**, Bax **(C)**, and Bcl2 **(D)** were determined using real-time PCR. The level of SOD2, CAT, and Bcl2 expression decreased significantly in the Mod group. After hUCMSC treatment, the expression of mRNA of antioxidant and anti-apoptotic genes increased significantly. Levels of expression increased more in the groups treated with hUCMSCs for 1 month than in those treated with hUCMSCs for 2 weeks. The levels of Bax increased in the Mod group and decreased in the IV-u 2m, IV-u 1m, and MI-u1m groups compared to the corresponding groups treated with PBS. The * symbol indicates the Mod group versus the NC group, groups treated with hUCMSCs versus corresponding groups treated with PBS, the MI-u1m group versus the IV-u1m group, or the MI-u2w group versus the IV-u2w group, *$p < 0.05$, **$p < 0.01$; The # symbol indicates the IV-u1m group versus the IV-u2w group or the MI-u1m group verus the MI-u2w group, #$p < 0.05$.



**Figure 8. Effect of hUCMSCs on the expression of antioxidant and anti-apoptotic proteins in mice ovaries. (A)** Representative Western blots of SOD2, CAT, Bax, and Bcl2 in the ovaries of mice. **(B-E)** The relative levels of expression of SOD2, CAT, Bax, and Bcl2 protein in each group. The level of expression of SOD2, CAT, and Bcl2 increased and the level of expression of Bax decreased in the IV-u1m, IV-u2w, and MI-u1m groups. The level of protein expression did not differ significantly in the MI-u2w or MI-p2w groups. The * symbol indicates the Mod group versus the NC group, groups treated with hUCMSCs versus corresponding groups treated with PBS, the MI-u1m group versus the IV-u1m group, or the MI-u2w group versus the IV-u2w group, *$p < 0.05$.

relative to the aging of other body systems, and ovarian aging is described as a gradual decline in the quantity and quality of ovarian follicles (*41*). The current study attempted to utilize continuous superovulation *via* repeated injections of PMSG, hCG, and PGF2α to accelerate the consumption of follicles as well as ozone inhalation to increase oxidative damage to the ovaries in order to create a model of accelerated ovarian in mice.

Once the model of accelerated ovarian aging was created, ovarian reserve diminished and the number of atretic follicles increased. Current evidence suggests that the estradiol level decreases relatively late in the process of ovarian aging and that the plasma level of progesterone does not change significantly (*42-44*). The current results indicated that the plasma levels of estradiol and progesterone decreased in the Mod group of mice. The estrous cycles of older mice were longer and then the capacity for maintaining cycles finally disappeared. Most of the vaginal lavages from acyclic mice were leukocytic (*i.e.* diestrus or metaestrus) (*45*). In the current study, the percentage of mice in the Mod group with irregular cycles and cycles that ceased increased markedly with a decrease in plasma levels
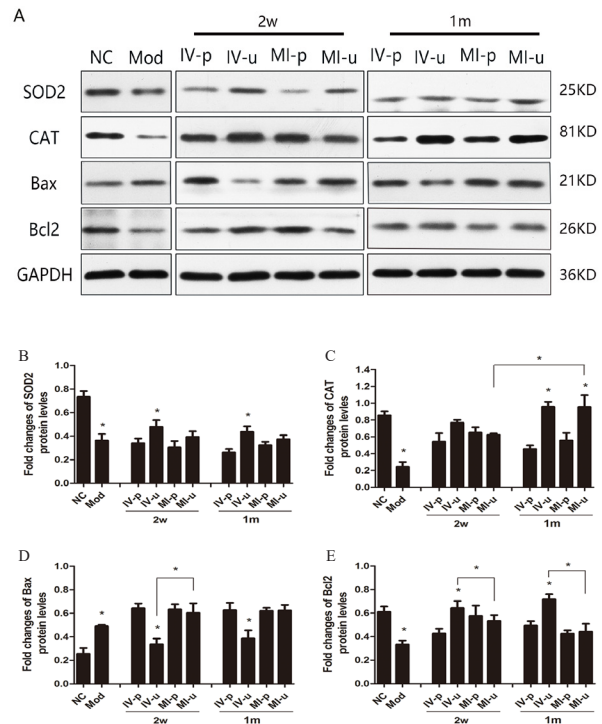
of estradiol and progesterone. Menstrual changes are therefore considered to be an early manifestation of ovarian dysfunction. A decrease in the follicle count with age indicates the onset of cycle irregularity and the final cessation of menses (*46,47*), which is the final step in the process of ovarian aging. Moreover, the corresponding age-related decline in oocyte quality is widely known to be a major impetus for low pregnancy rates in aging females. In the current study, fertility and fecundity declined markedly in the Mod group of mice.

The current results indicated that the plasma levels of estradiol and progesterone increased in the group treated with hUCMSCs for 1 month and the IV-u2w group. This finding may be due to the increase in normal healthy antral follicles and the decrease in atretic follicles. The percentage of regular cycles also increased after hUCMSC transplantation. A higher percentage of mice treated with hUCMSCs for 1 month exhibited regular cycles and higher numbers of newborns per litter. The current results indicated that transplantation *via* injection in the tail vein and treatment for 1 month are more suitable for restoration of ovarian function. In this study, both methods of transplantation yielded satisfactory results in terms

of restoring ovarian function, although these two approaches did differ significantly in some respects. Intravenous injection has several advantages over in situ ovarian micro injection. Intravenous injection is generally less invasive, it has more marked effects, and it can more effectively restore ovarian function.

After hUCMSC treatment, ovarian function in mice recovered as expected, although transplanted cells did not develop into follicle components. Apoptosis is likely to be a relevant mechanism in the process of ovarian aging (*48-50*). Previous studies have shown that stem cells can inhibit apoptosis through secretion of stanniocalcin-1 and paracrine factors and they can enhance the oxidative stress response pathway. Apoptosis generally increases to a very high level when mice are subjected to oxidative stress. After hUCMSC treatment, the number of TUNEL-positive cells decreased significantly, indicating that hUCMSCs can reduce apoptosis caused by superovulation and oxidative stress.

Reactive oxygen species (ROS) are considered to be an underlying factor for aging and may initiate aging by causing oxidative damage (*51*). Increased levels of endogenous ROS and diminished antioxidant defenses lead to a wide range of cellular oxidative damage, which includes a subsequent decrease in ovarian quality. The current results also indicated that ovarian expression of SOD2 and CAT decreased considerably compared to that in the NC group. After hUCMSC transplantation, expression of SOD2 and CAT increased in all groups except the MI-u 2w group. In the IV-u1m group of mice, the expression of SOD2 and CAT was markedly higher than that in the IV-u2w and MI-u1m groups. Thus, the observed effect was most probably due to enhanced expression of genes coding for antioxidant and anti-apoptotic enzymes.

Over the past few years, human MSCs have been extensively studied in clinical trials to treat various conditions such as neurological diseases, cardiovascular diseases, immune diseases, gastrointestinal diseases, and blood diseases. However, only a few studies have determined an optimal method for stem cell transplantation, at least in the field of reproductive medicine. The current study compared 2 general forms of stem cell therapy and findings revealed that IV, which is widely used in clinical settings, is more suitable to restoring ovarian function. Recent clinical studies have suggested that traditional Chinese medicines such as Kuntai capsules can effectively alleviate clinical symptoms, increase levels of estrogen, and decrease levels of follicle-stimulating hormone (FSH) and luteinizing hormone (LH) in the women with diminished ovarian reserve or premature ovarian failure (*52,53*). Traditional Chinese medicines are usually taken orally. Nonetheless, IV may be the best route for administration of traditional Chinese medicines. Regardless, a better understanding and proper use of hUCMSCs may offer hope to women with aging ovaries who wish to conceive.

**References**

1. Broekmans FJ, Knauff EA, te Velde ER, Macklon NS, Fauser BC. Female reproductive ageing: Current knowledge and future trends. Trends Endocrinol Metab. 2007; 18:58-65.
2. Djahanbakhch O, Ezzati M, Zosmer A. Reproductive ageing in women. J Pathol. 2007; 211:219-231.
3. Hansen KR, Knowlton NS, Thyer AC, Charleston JS, Soules MR, Klein NA. A new model of reproductive aging: The decline in ovarian non-growing follicle number from birth to menopause. Hum Reprod. 2008; 23:699-708.
4. McGee EA, Hsueh AJ. Initial and cyclic recruitment of ovarian follicles. Endocr Rev. 2000; 21:200-214.
5. Markström E, Svensson ECh, Shao R, Svanberg B, Billig H. Survival factors regulating ovarian apoptosis – dependence on follicle differentiation. Reproduction. 2002; 123:23-30.
6. te Velde ER, Pearson PL. The variability of female reproductive ageing. Hum Reprod Update. 2002; 8:141-154.
7. Block E. A quantitative morphological investigation of the follicular system in newborn female infants. Acta Anat (Basel). 1953; 17:201-206.
8. Alviggi C, Humaidan P, Howles CM, Tredway D, Hillier SG. Biological versus chronological ovarian age: Implications for assisted reproductive technology. Reprod Biol Endocrinol. 2009; 7:101.
9. te Velde ER, Scheffer GJ, Dorland M, Broekmans FJ, Fauser BC. Developmental and endocrine aspects of normal ovarian aging. Mol Cell Endocrinol. 1998; 145:67-73.
10. Faddy MJ, Gosden RG, Gougeon A, Richardson SJ, Nelson JF. Accelerated disappearance of ovarian follicles in mid-life: Implications for forecasting menopause. Hum Reprod. 1992; 7:1342-1346.
11. Sohal RS. Role of oxidative stress and protein oxidation in the aging process. Free Radic Biol Med. 2002; 33:37-44.
12. Tarín JJ.. Aetiology of age–associated aneuploidy: A mechanism based on the 'free radical theory of ageing'. Hum Reprod. 1995; 10:1563-1565.
13. Tarín JJ. Potential effects of age-associated oxidative stress on mammalian oocytes/embryos. Mol Hum Reprod. 1996; 2:717-724.
14. Tamura H, Takasaki A, Miwa I, Taniguchi K, Maekawa R, Asada H, Taketani T, Matsuoka A, Yamagata Y, Shimamura K, Morioka H, Ishikawa H, Reiter RJ, Sugino N. Oxidative stress impairs oocyte quality and melatonin protects oocytes from free radical damage and improves fertilization rate. J Pineal Res. 2008; 44:280-287.
15. Liu L, Keefe DL. Cytoplasm mediates both development and oxidation-induced apoptotic cell death in mouse

zygotes. Biol Reprod. 2000; 62:1828-1834.

16. Liu L, Trimarchi JR, Keefe DL. Involvement of mitochondria in oxidative stress-induced cell death in mouse zygotes. Biol Reprod. 2000; 62:1745-1753.

17. Lass A, Skull J, McVeigh E, Margara R, Winston RM. Measurement of ovarian volume by transvaginal sonography before ovulation induction with human menopausal gonadotrophin for in-vitro fertilization can predict poor response. Hum Reprod. 1997; 12:294-297.

18. Nabhan SK, Bitencourt MA, Duval M, *et al*. Fertility recovery and pregnancy after allogeneic hematopoietic stem cell transplantation in Fanconi anemia patients. Haematologica. 2010; 95:1783-1787.

19. Nagano M, Kimura K, Yamashita T, Ohneda K, Nozawa D, Hamada H, Yoshikawa H, Ochiai N, Ohneda O. Hypoxia responsive mesenchymal stem cells derived from human umbilical cord blood are effective for bone repair. Stem Cells Dev. 2010;19:1195-1210.

20. Bieback K, Kern S, Klüter H, Eichler H. Critical parameters for the isolation of mesenchymal stem cells from umbilical cord blood. Stem Cells 2004 ;22:625-634.

21. Ciavarella S, Dominici M, Dammacco F, Silvestris F. Mesenchymal stem cells: A new promise in anticancer therapy. Stem Cells Dev. 2011;20:1-10.

22. Fong CY, Chak LL, Biswas A, Tan JH, Gauthaman K, Chan WK, Bongso A. Human Wharton's jelly stem cells have unique transcriptome profiles compared to human embryonic stem cells and other mesenchymal stem cells. Stem Cell Rev. 2011;7:1-16.

23. Wang S, Yu L, Sun M, Mu S, Wang C, Wang D, Yao Y. The therapeutic potential of umbilical cord mesenchymal stem cells in mice premature ovarian failure. Biomed Res Int. 2013; 2013:690491.

24. Liu T, Huang Y, Guo L, Cheng W, Zou G. CD44^{+}/CD105^{+} human amniotic fluid mesenchymal stem cells survive and proliferate in the ovary long-term in a mouse model of chemotherapy-induced premature ovarian failure. Int J Med Sci. 2012; 9:592-602.

25. Takehara Y, Yabuuchi A, Ezoe K, Kuroda T, Yamadera R, Sano C, Murata N, Aida T, Nakama K, Aono F, Aoyama N, Kato K, Kato O. The restorative effects of adipose-derived mesenchymal stem cells on damaged ovarian function. Lab Invest.. 2013; 93:181-193.

26. Liu T, Huang Y, Zhang J, Qin W, Chi H, Chen J, Yu Z, Chen C. Transplantation of human menstrual blood stem cells to treat premature ovarian failure in mouse model. Stem Cells Dev. 2014; 23:1548-1557.

27. Miyamoto K, Sato EF, Kasahara E, Jikumaru M, Hiramoto K, Tabata H, Katsuragi M, Odo S, Utsumi K, Inoue M. Effect of oxidative stress during repeated ovulation on the structure and functions of the ovary, oocytes, and their mitochondria. Free Radic Biol Med. 2010; 49:674-681.

28. Rivas-Arancibia S, Guevara-Guzman R, Lopez-Vidal Y, Rodriguez-Martinez E, Zanardo-Gomes M, Angoa-Perez M, Raisman-Vozari R. Oxidative stress caused by ozone exposure induces loss of brain repair in the hippocampus of adult rats. Toxicol Sci. 2010; 113:187-197.

29. Feng R, He W, Ochi H. A new murine oxidative stress model associated with senescence. Mech Ageing Dev. 2001; 122:547-559.

30. Qi S, Wu D. Bone marrow-derived mesenchymal stem cells protect against cisplatin-induced acute kidney injury in rats by inhibiting cell apoptosis. Int J Mol Med.

2013;32:1262-1272.

31. Park JH, Hwang I, Hwang SH, Han H, Ha H. Human umbilical cord blood-derived mesenchymal stem cells prevent diabetic renal injury through paracrine action. Diabetes Res Clin Pract. 2012;98:465-473.

32. Latifpour M, Nematollahi-Mahani SN, Deilamy M, Azimzadeh BS, Eftekhar-Vaghefi SH, Nabipour F, Najafipour H, Nakhaee N, Yaghoubi M, Eftekhar-Vaghefi R, Salehinejad P, Azizi H. Improvement in cardiac function following transplantation of human umbilical cord matrix-derived mesenchymal cells. Cardiology. 2011;120:9-18.

33. Chang YS, Choi SJ, Ahn SY, Sung DK, Sung SI, Yoo HS, Oh WI, Park WS. Timing of umbilical cord blood derived mesenchymal stem cells transplantation determines therapeutic efficacy in the neonatal hyperoxic lung injury. PLoS One. 2013;8:e52419.

34. Tilly JL. Ovarian follicle counts - not as simple as 1, 2, 3. Reprod Biol Endocrinol. 2003; 1:11.

35. Marcondes FK, Bianchi FJ, Tanno AP. Determination of the estrous cycle phases of rats some helpful considerations. Braz J Biol. 2002; 62:609-614.

36. Schedin P, Mitrenga T, Kaeck M. Estrous cycle regulation of mammary epithelial cell proliferation, differentiation, and death in the Sprague-Dawley rat: A model for investigating the role of estrous cycling in mammary carcinogenesis. J Mammary Gland Biol Neoplasia. 2000; 5:211-225.

37. Yang S, Wang S, Luo A, *et al*. Expression patterns and regulatory functions of microRNAs during the initiation of primordial follicle development in the neonatal mouse ovary. Biol Reprod. 2013; 89:126.

38. Aerts JL, Christiaens MR, Vandekerckhove P. Evaluation of progesterone receptor expression in eosinophils using real-time quantitative PCR. Biochim Biophys Acta. 2002; 1571:167-172.

39. Zhang J, Fang L, Lu Z, Xiong J, Wu M, Shi L, Luo A, Wang S. Are sirtuins markers of ovarian aging? Gene. 2016; 575:680-686.

40. Perheentupa A, Huhtaniemi I. Aging of the human ovary and testis. Mol Cell Endocrinol. 2009; 299:2-13.

41. Younis JS. Ovarian aging and implications for fertility female health. Minerva Endocrinol. 2012; 37:41-57.

42. Mersereau JE, Evans ML, Moore DH, Liu JH, Thomas MA, Rebar RW, Pennington E, Cedars MI. Luteal phase estrogen is decreased in regularly menstruating older women compared with a reference population of younger women. Menopause. 2008; 15:482-486.

43. Lee SJ, Lenton EA, Sexton L, Cooke ID. The effect of age on the cyclical patterns of plasma LH, FSH, oestradiol and progesterone in women with regular menstrual cycles. Hum Reprod. 1988; 3:851-855.

44. Muttukrishna S, Child T, Lockwood GM, Groome NP, Barlow DH, Ledger WL. Serum concentrations of dimeric inhibins, activin A, gonadotrophins and ovarian steroids during the menstrual cycle in older women. Hum Reprod. 2000; 15:549-556.

45. Nelson JF, Gosden RG, Felicio LS. Effect of dietary restriction on estrous cyclicity and follicular reserves in aging C57BL/6J mice. Biol Reprod. 1985; 32:515-522.

46. Broekmans FJ, Soules MR, Fauser BC. Ovarian aging: Mechanisms and clinical consequences. Endocr Rev. 2009; 30:465-493.

47. Soules MR, Sherman S, Parrott E, Rebar R, Santoro N, Utian W, Woods N. Executive summary: Stages of

Reproductive Aging Workshop (STRAW). Climacteric. 2001; 4:267-272.

48. Souidi N SM, Seifert M. Ischemia-reperfusion injury: Beneficial effects of mesenchymal stromal cells. Curr Opin Organ Transplant. 2013;18:34-43.

49. Lin H, Xu R, Zhang Z, Chen L, Shi M, Wang FS. Implications of the immunoregulatory functions of mesenchymal stem cells in the treatment of human liver diseases. Cell Mol Immunol. 2011;8:19-22.

50. Yan Y, Xu W, Qian H, Si Y, Zhu W, Cao H, Zhou H, Mao F. Mesenchymal stem cells from human umbilical cords ameliorate mouse hepatic injury *in vivo*. Liver Int. 2009;29:356-365.

51. Harman D. The free radical theory of aging. Antioxid Redox Signal. 2003; 5:557-561.

52. Chen JM, Gao HY, Ding Y, Yuan X, Wang Q, Li Q, Jiang GH. Efficacy and safety investigation of Kuntai capsule for the add-back therapy of gonadotropin releasing hormone agonist administration to endometriosis patients: a randomized, double-blind, blank- and tibolone-controlled study. Chin Med J (Engl). 2015;128:427-432.

53. Liu, CQ, Qin ZX, Jiang FF, Hong T, Wang F. Kuntai capsule combined with gonadotropin releasing hormone agonist in treatment of moderate-severe endometriosis: A clinical observation. Zhongguo Zhong Xi Yi Jie He Za Zhi. 2014; 34:1288-1291. (in Chinese)